Laser Ablation of Titanium Alloy (Ti64): Effects of Process Parameters on Performance of Laser Welded Ti64 – Polyamide 6.6 Joints.

Adham Al-Sayyad (adham.alsayyad@uni.lu)
Universite du Luxembourg https://orcid.org/0000-0002-0254-3610

Farah Salah
Laser Ablation of Titanium Alloy (Ti64): Effects of Process Parameters on Performance of Laser Welded Ti64 – Polyamide 6.6 Joints.

Julien Bardon
Luxembourg Institute of Science and Technology, L4362 Esch-sur-Alzette, Luxembourg

Pierre Hirchenhahn
University of Namur

Lamia Shihata
German University in Cairo

Laurent Houssiau
University of Namur

Peter Plapper
Universite du Luxembourg

Research Article

Keywords: Laser welding, metal - polymer joints, laser ablation, Design of Experiments

Posted Date: February 24th, 2021

DOI: https://doi.org/10.21203/rs.3.rs-219911/v1

Laser ablation of titanium alloy (Ti64): effects of process parameters on performance of laser welded Ti64 – polyamide 6.6 joints.

Adham Al-Sayyad *[1], Farah Salah [2], Julien Bardon [3], Pierre Hirchenhahn [4], Lamia A. Shihata [2], Laurent Houssiau [4] and Peter Plapper [1]

[1] Faculty of Science, Technology and Medicine (FSTM), University of Luxembourg, L1359 Luxembourg, Luxembourg
[2] Faculty of Engineering and Material Science, German University in Cairo, 11835 Cairo, Egypt
[3] Materials Research and Technology (MRT), Luxembourg Institute of Science and Technology, L4362 Esch-sur-Alzette, Luxembourg
[4] LISE laboratory, Namur Institute of Structured Materials (NISM), University of Namur, 5000 Namur, Belgium
* Correspondence: adham.alsayyad@uni.lu; Tel.: +352-466-644-6034

Keywords: Laser welding; metal - polymer joints; laser ablation; Design of Experiments

Abstract

Laser welding of metals – polymers has gained strong scientific and industrial interest because of its ability to produce miniaturized joints in lightweight products with customized properties. Surface pretreatments before joining process have shown significant impact on enhancing properties of laser welded metal – polymer joints. This work adopts a Design of Experiments (DoE) approach to investigate the influence of titanium alloy (Ti64) laser ablation parameters on the performance of laser welded Ti64 – polyamide (PA6.6) assemblies. In this first study, significant laser ablation parameters were highlighted, process window outlined, and optimal parameters identified. Laser ablation pretreatment parameters demonstrated a strong influence on joint resistance to failure. Effects of laser ablation parameters on titanium surface morphology were analyzed using Scanning Electron Microscope (SEM). In a second study, the effects of ablation parameters on Ti64 surface properties and welding quality will be investigated.

Introduction

Joining of metals to polymers is important for developing lightweight components with tailored properties. The joining of titanium alloy (Ti64) to polyamide (PA6.6) is relevant for automotive, aerospace, marine, and even biomedical applications, where both materials are commonly used [1–6]. The most frequently used metal – polymer joining techniques are adhesive bonding and mechanical fastening. Both techniques necessitate an overlapping joint configuration to achieve the required joint strength. However, adhesive bonding generally requires long curing time and involves hazardous materials, whereas mechanical fastening adds extra weight, geometrical constraints, and stress concentration points to the

assembly [7,8]. Therefore, laser beam welding is a favorable joining alternative as a rapid and low energy process, providing reliable and lightweight joints.

Thermal joining of metals to polymers is challenging because of the significant difference of the thermal properties and melting temperatures of both materials. However, focused laser beam energy provides a contactless thermal joining solution for joining metals to polymers by allowing a finely controlled introduction of energy into the materials, yielding a high temperature gradient in a limited volume. This precise control over the heat input provides the opportunity to thoroughly melt the polymer at the interface of the joint while, at the same time, avoiding its degradation [9,10]. To model the effects of laser welding parameters and optimize the joining process, previous work demonstrated the successful use of DoE techniques for laser joining of Ti64 to PA6.6 [11] and carbon fiber reinforced PA6.6 [12].

Surface pretreatment of metals, prior to thermal joining with polymers, has shown significant impact on improving performance of assemblies. Researchers [13–15] analyzed effects of mechanical and chemical pretreatments for metals on strength of thermally joined metal – polymer assemblies. The use of a laser beam for metallic surface pretreatment is favored over chemical and mechanical pretreatments as a rapid, solventless and contactless process, which can be easily automated. Effects of laser surface structuring on metals, using Nd:YAG laser, before laser welding and thermal joining to selected polymers were examined [16–19]. The modified surface chemistry along with the structuring allowed for enhanced chemical bonding and mechanical interlocking at the interface between joining. This was for instance the case for Holtkamp et. al. [17], who reported a correlation between increased shear strength and laser surface structural density (per unit area). Otherwise, Al-Sayyad et.al. [20] utilized DoE techniques to investigate effects of aluminum laser ablation pretreatment parameters, using short (ns) pulsed laser, on performance of laser welded aluminum to PA6.6. Results highlighted the significance of pulse frequency and beam guidance speed on the performance. Furthermore, they demonstrated strong impact of laser ablated aluminum surface topography on the interfacial thermal transfer when laser welding to PA6.6, affecting joint area and mechanical performance [21].

Researchers [22–28] investigated the effects of Ti64 surface pretreatment, by means of laser beam source, on the strength of adhesive bonded metal – polymer joints. Results highlight impact of laser pretreatment on improving joint strength by enhancing interfacial chemical bonding and mechanical interlocking. Moreover, Chanthapan et.al. [29] investigated the effects of titanium oxide layer on the strength and durability of laser welded titanium polyamide joints. However, laser treatment of Ti64 prior

to laser welding with polymers has been neglected in literature and the effects of laser pretreatment parameters on joint behaviors remain unclear.

The objective of the present study is twofold. First, it is complementary to article [11] by utilizing laser ablation in order to further increase the joint resistance of Ti64-PA66 assemblies. Even with their high industrial relevance, such assemblies obtained by laser welding are seldom reported in literature [12], and the aim of the authors is to show the performance of an all-laser process - Ti64 laser ablation pretreatment and laser welding with PA66 - to obtain high level of mechanical resistance for Ti64-PA66 assemblies. Second, the present study aims at identifying the best laser pretreatment parameters values to reach a good welding quality. In a second part to be published afterwards, the effects of ablation parameters on Ti64 surface properties will be evaluated and the link of this surface characteristics with welding quality will be investigated.

Experimental methods

Using DoE techniques, this work investigates the effects of laser ablation on the shear resistance to failure of laser welded Ti64 to PA6.6. The influence of laser ablation parameters on surface morphology of selected samples was investigated using Scanning Electron Microscopy (SEM).

2.1 Materials

In those experiments, 0.5 mm thick titanium alloy Ti-6Al-5V (Ti64) purchased from E. Wagener GmbH (Weissach-Flacht, Germany), with geometry of 30 mm× 60 mm, and 4 thick mm polyamide 6.6 (PA6.6) purchased from Dutec (Ahaus, Germany), with the dimensions of 25 mm × 75 mm were used. The elemental composition of Ti64 is shown in Table 1. Prior to the joining process, Ti64 samples were prepared by laser ablation, and PA samples were wiped with ethanol, to remove potential surface contaminants.

Table 1: Elemental composition of Ti64

Element	Fe	C	N	H	O	Al	V	Ti
Atomic weight %	0.18	0.014	0.009	0.0094	0.132	6.12	4.28	rest

2.2 Laser welding

Ti64 and PA6.6 were joined by a laser beam welding using a fiber laser (Tru-Fiber 400 from TRUMF) as indicated by the optimized parameters from the authors' previous research [11]. The laser had a wavelength of 1070 nm and a spot size of 31 µm. Figure 1 shows the welding setup with joining partners clamped in an overlap welding arrangement. The laser beam was focused and irradiated on the titanium

surface where part of the laser beam energy is absorbed and conducted to the joint interface in the form of heat energy, causing the polymer to melt and bond to titanium. In order to widen the weld path, the laser beam followed a spiral wobble trajectory. Argon shielding gas with flowrate of 10L/min was targeted at the weld zone, with 20° inclination angle below the horizontal, to prevent interaction of titanium with atmosphere.

To evaluate the strength of the welded joint, single lap shear test was performed using Z010 from Zwick/Roell which has maximum load of 10 KN. The crosshead pulling speed was set at 1.2 mm/min. Samples were clamped in a vertical alignment with a jaw to jaw distance of 75 mm.

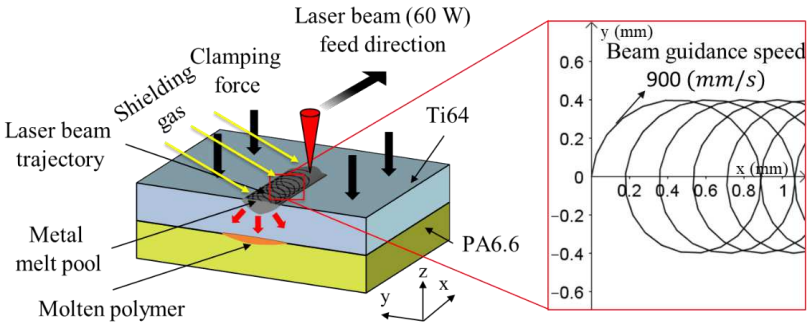

Figure 1: Laser welding setup

2.3 Laser ablation DoE

Titanium surface at the joining partners' interface was ablated prior to the joining process by irradiating it with short pulsed (ns) Nd:YVO4 laser (TruMark 6130 from TRUMPF) having a wavelength of 1064 nm. While the pulse frequency affects the Peak Pulse Power (PPP), the pulses overlap ratio (O), shown in Figure 2 (a) and described by Equation 1, is influenced by three parameters: pulse frequency (fp), beam diameter (Ø) and beam deflection speed (V). Keeping a constant beam diameter of 45 µm, and independently decreasing the pulse frequency or increasing the beam speed results in a decrease in the overlap ratio. Hence, a combination of both parameters, among others, can produce different surface structures as shown in Figure 2.

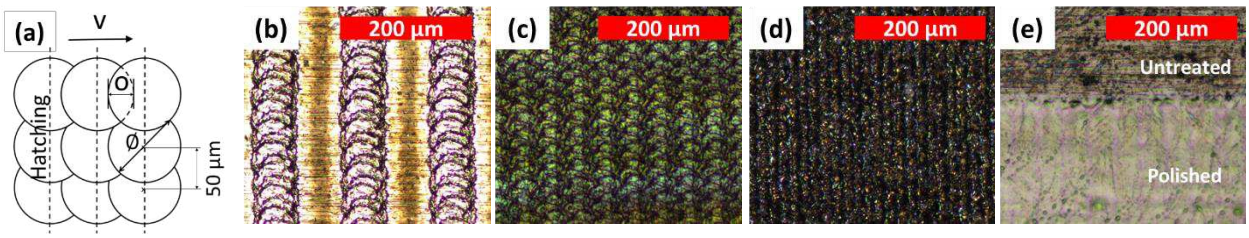

Figure 2: (a) schematic showing ablation parameters on Ti64 surface; (b) patterned ablation; (c) semi-patterned ablation; (d) stochastic ablation; (d) polished ablation.

$$O\ (\%) = \left(1 - \frac{V\ (\frac{mm}{s})}{\emptyset\ (mm) \times f_p\ (Hz)}\right) \times 100 \quad (1)$$

2.3.1 Screening DoE

In order to identify the most significant ablation parameters affecting the joint behavior, Plackett-Burman method [30] was utilized with the aid of Minitab® software. Six factors were screened as shown in Table 2 below. Two levels were chosen per factor. Preliminary investigations were done to determine the high and low levels of each factor in order to ensure adequate weld for all possible parametric combinations. 24 experimental runs were designed to investigate the significance of the six parameters with a relatively high statistical power of 80% chance detecting a standard deviation of 1.06. Spot size describes the one on the titanium surface during the laser ablation process. Focusing on the surface of titanium results in a spot size of 45 µm, and defocusing with a downward offset of 2.5 mm results in spot size of 102 µm on titanium surface. Pulse frequency along with the power percentage influence the Peak Pulse Power (PPP), and the beam speed together with the pulse frequency and the spot size influence the overlap ratio. The hatching parameter presents orientation of laser structured lines with reference to the direction of the applied shear load. Argon shielding gas with volumetric flow rate of 10 L/min was used to investigate effects of shielding treated titanium surface from the atmosphere on the joint behavior. After the ablation, the welding process took place as described in section 2.2.

Table 2: Screening parameters

Factors	Data Type	Low level	High level
Spot size (µm)	Continuous	45	102
Pulse frequency (kHz)	Continuous	15	120
Speed (mm/s)	Continuous	1000	2500
Power %	Continuous	10	70
Hatching	Categorical	Parallel	Perpendicular
Shielding gas	Categorical	Off	On

2.3.2 Optimization DoE

After highlighting the most significant parameters affecting joint resistance to failure, influential parameters were varied simultaneously by implementing a Central Composite Design (CCD), with a total samples of 8 cube points, 5 center points, and 8 axial points, in order to outline the process window using Response Surface Method (RSM) [31]. Domain of variation of RSM design was set to two coded units. Mathematical model was generated to describe the effect of those ablation parameters, and their

interaction, on the joint's resistance to failure using ANOVA technique [32]. In order to expand the investigated process window, further tests were performed along the path of steepest ascent as well as the path of optimal overlap ratio as determined solving the generated model. Path of steepest ascent utilized four steps. Preliminary investigations recommended large step size to be able to detect significant difference in joint behavior. Thus, pulse frequency was used as a base factor, and a step size of two coded units was used between first three steps, and four coded units between the third and fourth step. 56 samples in total were tested for the complete optimization process.

2.4 Scanning Electron Microscope (SEM)

SEM was performed on treated Ti64 surfaces using a pressure-controlled FEI Quanta FEG 200 scanning electron microscope from FEI Company (Hillsboro, OR, USA). Measurements were carried out in secondary electron mode to get information about the samples' morphology. The test was performed under a high vacuum with a 20 kV acceleration voltage. In order to investigate effects of ablation parameters on surface morphology and corresponding influence on joint performance, five regions of 1 cm^2 area were ablated on a Ti64 sample with varied parameters that resulted in a wide range of joint resistance to failure.

3. Results and Discussion

3.1 Screening DoE

Screening design resulted in several surface structures, including patterned, semi-patterned, stochastic, and polished (Figure 2). Polishing effect was only achievable at relatively high pulse frequency (120 kHz) and low PPP (5 kW). Visual investigation showed mixed cohesive/adhesive failure mode in the case of the polished titanium surface, and only cohesive failure mode in the rest of the ablated surface structures welded to PA6.6. Pareto chart (Figure 3) illustrates the magnitude of effects of the screened parameters. The effect of a single parameter demonstrates the difference in mean shear load at its high and low values. The dotted red line shows the effect size at 0.05 level of significance as determined by Lenth's method [33]. Results identified only pulse frequency to have statistical significance on the achieved shear load. Figure 3 shows the main effect plot, which describes how changes to a single factor affect the mean shear load. Results show that a low level of the pulse frequency is favored to increase the shear load, explaining the low joint resistance to failure in the case of polished samples. However, the pulse frequency has an influence on both the overlap ratio and PPP. Thus, it was decided to proceed with the optimization process by simultaneously varying both pulse frequency and beam speed in order to have independent control over the overlap ratio and PPP (see section 2.3).

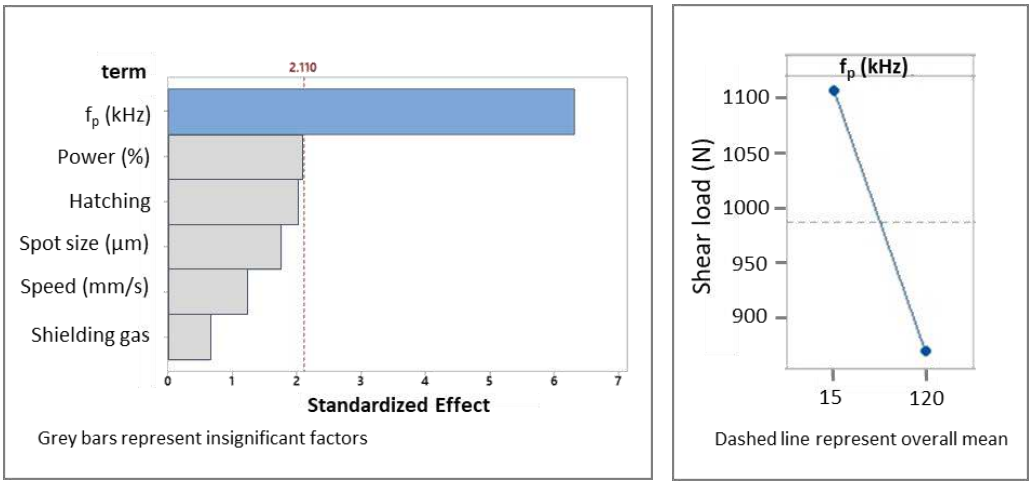

Figure 3: (left) Pareto chart; (right) main effect plot

3.2 Optimization DoE

Pulse frequency and beam speed were used to create a predictive model while keeping the rest of the parameters constant as shown in Figure 4.

Figure 4 shows the contour plot of the developed regression model (Equation 2). The red dots represent the CCD testing conditions. ANOVA analysis shows high accountability of the model (coefficient of determination R^2 = 93.8% and the significance of its coefficients (p-value < 0.05), in particular: pulse frequency, beam speed, and non-linearity in speed. ANOVA analysis showed a significant impact of beam speed (V [mm/s]), and significant non-linearity in its response (V^2), with no significant impact of pulse frequency (fp [kHz]) and no interaction between pulse frequency and speed. Dashed lines shown on the contour plot indicate overlap ratio generated by the combination of pulse frequency and speed. Results show significant correlation between the overlap ratio and the contour lines, signifying the impact of overlap ratio on the joint's resistance to failure. Solving the regression model (equation 2) results in 1222 N as maximum predicted joint resistance to failure at 43.89 kHz and 364.15 mm/s, which corresponds to 82% overlap ratio.

In order to expand the process window, further tests were conducted by varying PPP at 82% overlap ratio in addition to following the steepest path of ascent. Figure 5 shows effects of expanding process window at 82% overlap ratio. Results indicate an increase in the direction of reducing PPP before a sharp drop in resulted shear load was identified at 5 kW. Although relatively large step size was used as elaborated in section 2.3.2, results illustrated in Figure 5 show slight increase of joint's resistance to failure, followed by slight decrease, along the path of steepest ascent reaching up to -790% overlap ratio (patterned

structure). The highest average load (1201 ± 35 N) is reached for 30.28 kHz and 5520.5 mm/s in pulse frequency and speed, respectively. However, 34.17 kHz and 3772.82 mm/s (PPP = 44.5 kW and O = -145%) resulted in smallest deviation in joint resistance to failure (1187 ± 11 N). Thus, those latter parameters were identified as the optimal ablation conditions.

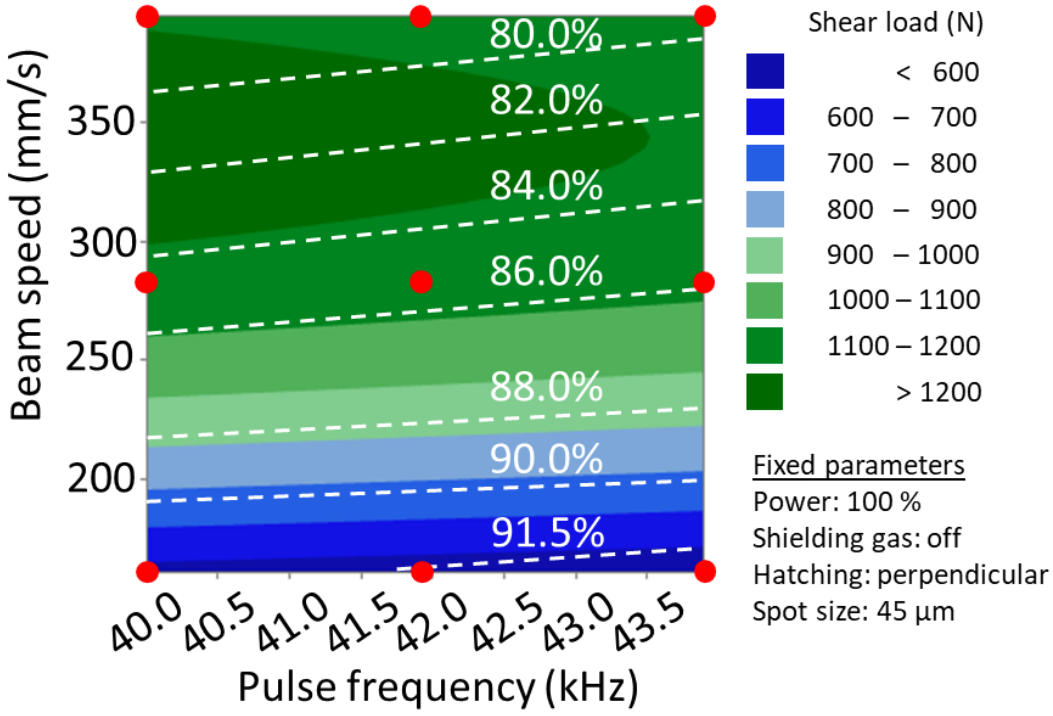

Figure 4: Contour plot of shear load as a function of beam speed and pulse frequency.

$$\text{Load (N)} = -654 - 11.6\,Fp + 13.71\,\text{V} - 0.01993\,\text{V}^2 \quad (2)$$

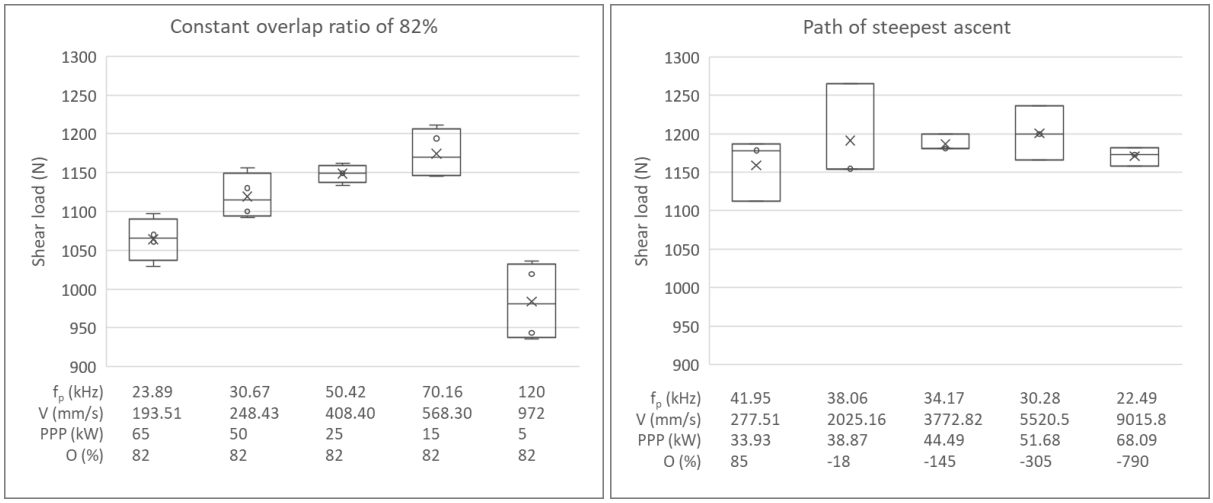

Figure 5: Expanding process window along: (left) 82% overlap ratio; (right) path of steepest ascent

3.3 Scanning Electron Microscope (SEM)

Figure 6 shows results of selected ablation parameters on morphology of treated titanium, and corresponding effects on joint resistance to failure. While ablation parameters of samples F1 to F4 are included in the optimization design, and the polished sample is included in the screening design, the reference sample is investigated separately with a surface only wiped with ethanol. It is well known in literature that laser ablation parameters, as well as laser-material interaction, has a strong influence on aspect-ratio and morphology of laser-induced craters [34–37]. Figure 6 shows that laser ablation process results in a differently sized laser-induced crater than the laser beam spot size irradiated on the treated surface (45 µm), which was used for calculating overlap ratio. As a result, ablated samples F1 – F4 demonstrate a larger actual overlap ratio of ablated spots compared to the calculated one, demonstrating semi-patterned to stochastic ablation geometries, which is reported throughout this article.

Visual inspection revealed mixture of cohesive/adhesive failure modes in the polished samples after joint failure, and purely cohesive failure mode at PA6.6 close to the weld zone in other cases of ablated titanium. Apart from the polished sample, which resulted in mixed cohesive/adhesive failure mode, qualitative assessment of the results shows that a “smoother” ablated surface is favorable for an increased joint resistance to failure. This can be due to the enhanced interfacial thermal transfer of smoother surfaces as reported with the case of ablated aluminum, which is laser welded to polyamide (PA6.6) [21]. Further investigations are currently on-going and will be soon published as a second part of this study by the same authors.

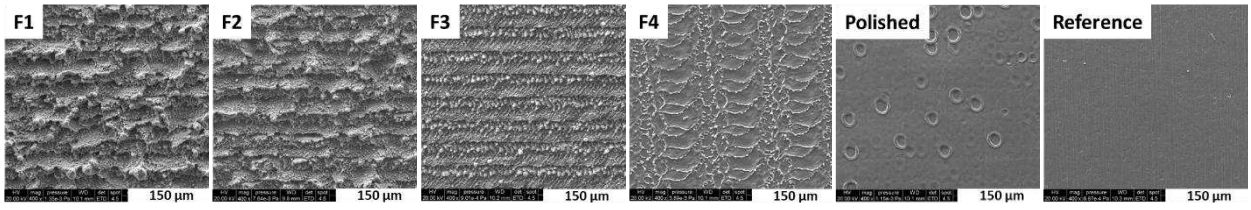

Shear load (N)	387 ± 117	690 ± 57	1064 ± 28	1186 ± 11	764 ± 5	772 ± 70
Fp (kHz)	43.89	40.00	23.89	34.17	120.00	-
V (mm/s)	160.00	160.00	193.50	3772.82	2500.00	-
PPP (kW)	32.00	37.37	65.00	41.70	5.00	-
O (%)	91.89	91.11	82.00	-145.00	53.01	-

Figure 6: effects of ablation parameters on morphology of Ti64 surface

4. Conclusion

Design of experiments was developed to inspect the influence of laser ablation parameters, using short (ns) pulsed laser, on the joint quality and resistance to failure of Ti64 laser welded to PA6.6. From the screening process, it was concluded that the most significant factor is the pulse frequency which is

responsible for Peak Pulse Power and pulse overlap ratio. Using Response Surface Method (RSM), statistically significant regression model was developed to describe relation between pulse frequency and beam speed on the joint's resistance to failure. Results showed strong correlation between overlap ratio and joint's resistance to failure, predicting highest response of shear load at 82% overlap ratio within the investigated process window. Two further steps were carried out. One by following the path of steepest ascent and another one by expanding the process window at 82% overlap. The former step allowed to identify optimal ablation conditions at 34.17 kHz and 3772.82 mm/s (PPP = 44.5 kW and O = -145%) resulting in relatively highest joint resistance to failure and lowest deviation (1186 ± 11 N). SEM qualitative investigations show that a smoother ablated titanium surface was favorable for an increased joint resistance to failure. Enhanced interfacial thermal transfer with smoother ablated surface might explain this behavior. Further investigations are currently ongoing and will be reported in a future article.

Declaration

Funding

Authors would like to acknowledge FNR (Luxembourg), and DGO6 (Walloon region, Belgium) for financially supporting this research work through the LaserSTAMP project.

Conflicts of interest/Competing interests

The authors have no conflicts of interest to disclose

Availability of data and material

Raw data were generated at the University of Luxembourg. Derived data supporting the findings of this study are available from the corresponding author on request.

Code availability

Not applicable

References

[1] I. Inagaki, T. Takechi, S. Yoshihisa, A. Nozomu, Application and Features of Titanium for the Aerospace Industry, Nippon steel & Sumitomo metal technical report (2014) 22-27.

[2] R.R. Boyer, Titanium for aerospace: Rationale and applications, Adv. Perform. Mater. 2 (1995) 349–368. https://doi.org/10.1007/BF00705316.

[3] G. Renganathan, N. Tanneru, S.L. Madurai, Orthopedical and biomedical applications of titanium and zirconium metals, in: P. Balakrishnan, S.M. S, S. Thomas (Eds.), Fundam. Biomater. Met., Woodhead Publishing, 2018: pp. 211–241. https://doi.org/10.1016/B978-0-08-102205-4.00010-6.

[4] C.N. Elias, J.H.C. Lima, R. Valiev, M. A. Meyers, Biomedical Applications of Titanium and its Alloys, J. Miner. Met. Mater. Soc. (2008) 46–49. https://doi.org/10.1007/s11837-008-0031-1.

[5] M. Vojdani, R. Giti, Polyamide as a Denture Base Material: A Literature Review., J. Dent. (Shiraz, Iran). 16 (2015) 1–9.

[6] J.R. Davis, Handbook of Materials for Medical Devices, 2003. https://doi.org/10.1361/hmmd2003p001.

[7] P. Kah, R. Suoranta, J. Martikainen, C. Magnus, Techniques for joining dissimilar materials: Metals and polymers, Rev. Adv. Mater. Sci. 36 (2014) 152–164.

[8] H.L. Gower, R.R.G.M. Pieters, I.M. Richardson, Pulsed laser welding of metal-polymer sandwich materials using pulse shaping, J. Laser Appl. 18 (2006) 35–41. https://doi.org/10.2351/1.2080307.

[9] S. Katayama, Y. Kawahito, M. Mizutani, Latest Progress in Performance and Understanding of Laser Welding, Phys. Procedia. 39 (2012) 8–16. https://doi.org/10.1016/j.phpro.2012.10.008.

[10] K. Schricker, J. Pierre Bergmann, Determination of sensitivity and thermal efficiency in laser assisted metal-plastic joining by numerical simulation, Procedia CIRP. 74 (2018) 511–517. https://doi.org/10.1016/j.procir.2018.08.133.

[11] A. Al-Sayyad, P. Lama, J. Bardon, P. Hirchenhahn, L. Houssiau, P. Plapper, Laser joining of titanium alloy to polyamide: influence of process parameters on the joint strength and quality, Int. J. Adv. Manuf. Technol. 107 (2020) 2917–2925. https://doi.org/10.1007/s00170-020-05123-1.

[12] Y. Cai, C. Huang, H.X. Liu, D.D. Meng, Y.W. Wu, X. Wang, Modeling and Optimization of Laser Direct Joining Process Parameters of Titanium Alloy and Carbon Fiber Reinforced Nylon Based on Response Surface Methodology, Key Eng. Mater. 620 (2014) 3–9. https://doi.org/10.4028/www.scientific.net/KEM.620.3.

[13] J.P. Bergmann, M. Stambke, Potential of laser-manufactured polymer-metal hybrid joints, Phys. Procedia. 39 (2012) 84–91. https://doi.org/10.1016/j.phpro.2012.10.017.

[14] Z. Zhang, J.G. Shan, X.H. Tan, J. Zhang, Effect of anodizing pretreatment on laser joining CFRP to aluminum alloy A6061, Int. J. Adhes. Adhes. 70 (2016) 142–151. https://doi.org/10.1016/j.ijadhadh.2016.06.007.

[15] A. Klotzbach, M. Langer, R. Pautzsch, J. Standfuß, E. Beyer, Thermal direct joining of metal to fiber reinforced thermoplastic components, 022421 (2017). https://doi.org/10.2351/1.4983243.

[16] P. Amend, S. Pfindel, M. Schmidt, Thermal joining of thermoplastic metal hybrids by means of mono- and polychromatic radiation, Phys. Procedia. 41 (2013) 98–105.

https://doi.org/10.1016/j.phpro.2013.03.056.

[17] J. Holtkamp, A. Roesner, A. Gillner, Advances in hybrid laser joining, Int. J. Adv. Manuf. Technol. 47 (2010) 923–930. https://doi.org/10.1007/s00170-009-2124-6.

[18] A. Roesner, S. Scheik, A. Olowinsky, A. Gillner, U. Reisgen, M. Schleser, Laser assisted joining of plastic metal hybrids, Phys. Procedia. 12 (2011) 373–380. https://doi.org/10.1016/j.phpro.2011.03.146.

[19] A. Al-Sayyad, J. Bardon, P. Hirchenhahn, G. Mertz, C. Haouari, L. Houssiau, P. Plapper, Influence of laser ablation and plasma surface treatment on the joint strength of laser welded aluminum-polyamide assemblies., in: JNPLI 2017, 2017.

[20] A. Al-Sayyad, J. Bardon, P. Hirchenhahn, K. Santos, L. Houssiau, P. Plapper, Aluminum pretreatment by a laser ablation process: influence of processing parameters on the joint strength of laser welded aluminum – polyamide assemblies, Procedia CIRP. 74 (2018) 495–499. https://doi.org/10.1016/j.procir.2018.08.136.

[21] A. Al-Sayyad, J. Bardon, P. Hirchenhahn, R. Vaudémont, L. Houssiau, P. Plapper, Influence of aluminum laser ablation on interfacial thermal transfer and joint quality of laser welded aluminum-polyamide assemblies, Coatings. 9 (2019). https://doi.org/10.3390/coatings9110768.

[22] M. Chérif, C. Loumena, J. Jumel, R. Kling, Performance of Laser Surface Preparation of Ti6Al4 v, Procedia CIRP. 45 (2016) 311–314. https://doi.org/10.1016/j.procir.2016.02.354.

[23] A. Kurtovic, E. Brandl, T. Mertens, H.J. Maier, Laser induced surface nano-structuring of Ti-6Al-4V for adhesive bonding, Int. J. Adhes. Adhes. 45 (2013) 112–117. https://doi.org/10.1016/j.ijadhadh.2013.05.004.

[24] T. Mertens, F.J. Gammel, M. Kolb, O. Rohr, L. Kotte, S. Tschöcke, S. Kaskel, U. Krupp, Investigation of surface pre-treatments for the structural bonding of titanium, Int. J. Adhes. Adhes. 34 (2012) 46–54. https://doi.org/10.1016/j.ijadhadh.2011.12.007.

[25] L.M. Galantucci, A. Gravina, G. Chita, M. Cinquepalmi, Surface treatment for adhesive-bonded joints by excimer laser, Compos. Part A Appl. Sci. Manuf. 27 (1996) 1041–1049. https://doi.org/10.1016/1359-835X(96)88890-7.

[26] E.G. Baburaj, D. Starikov, J. Evans, G.A. Shafeev, A. Bensaoula, Enhancement of adhesive joint strength by laser surface modification, Int. J. Adhes. Adhes. 27 (2007) 268–276. https://doi.org/10.1016/j.ijadhadh.2006.05.004.

[27] P. Maressa, L. Anodio, A. Bernasconi, A.G. Demir, B. Previtali, Effect of surface texture on the adhesion performance of laser treated Ti6Al4V alloy, J. Adhes. 91 (2014) 518–537.

https://doi.org/10.1080/00218464.2014.933809.

[28] S. Zimmermann, U. Specht, L. Spieß, H. Romanus, S. Krischok, M. Himmerlich, J. Ihde, Improved adhesion at titanium surfaces via laser-induced surface oxidation and roughening, Mater. Sci. Eng. A. 558 (2012) 755–760. https://doi.org/10.1016/j.msea.2012.08.101.

[29] S. Chanthapan, P. Wattanapornphan, C. Phongphisutthinan, Y. Kawahito, T. Suga, Effects of oxide layer on adhesion and durability of titanium and transparent polyamide joint by laser joining, J. Laser Appl. 30 (2018) 042005. https://doi.org/10.2351/1.5038052.

[30] R.L. Plackett, J.P. Burman, The design of optimum multifactorial experiments, Biometrika. 33 (1946) 305–325.

[31] G.E.P. Box, K.B. Wilson, On the Experimental Attainment of Optimum Conditions BT - Breakthroughs in Statistics: Methodology and Distribution, in: Break. Stat., 1992. https://doi.org/10.1007/978-1-4612-4380-9_23.

[32] R.H. Myers, D.C. Montgomery, C.M. Anderson-Cook, Response Surface Methodology Process and Product Optimization Using Designed Experiments, 4th Edition, 2016.

[33] R. V Lenth, Quick and Easy Analysis of Factorials Unreplicated, Technometrics. 31 (1989) 469–473.

[34] N. Maharjan, W. Zhou, Y. Zhou, Y. Guan, Ablation morphology and ablation threshold of Ti-6Al-4V alloy during femtosecond laser processing, Appl. Phys. A Mater. Sci. Process. 124 (2018) 1–10. https://doi.org/10.1007/s00339-018-1928-3.

[35] C. Zwahr, R. Helbig, C. Werner, A.F. Lasagni, Fabrication of multifunctional titanium surfaces by producing hierarchical surface patterns using laser based ablation methods, Sci. Rep. 9 (2019) 1–13. https://doi.org/10.1038/s41598-019-43055-3.

[36] B. Zheng, G. Jiang, W. Wang, K. Wang, X. Mei, Ablation experiment and threshold calculation of titanium alloy irradiated by ultra-fast pulse laser, AIP Adv. 4 (2014). https://doi.org/10.1063/1.4867088.

[37] M.A. Jafarabadi, M.H. Mahdieh, Evaluation of Crater Width in Nanosecond Laser Ablation of Ti in Liquids and the Effect of Light Absorption by Ablated Nano-Particles, Int. J. Opt. Photonics. 7 (2013) 105–112.

Figures

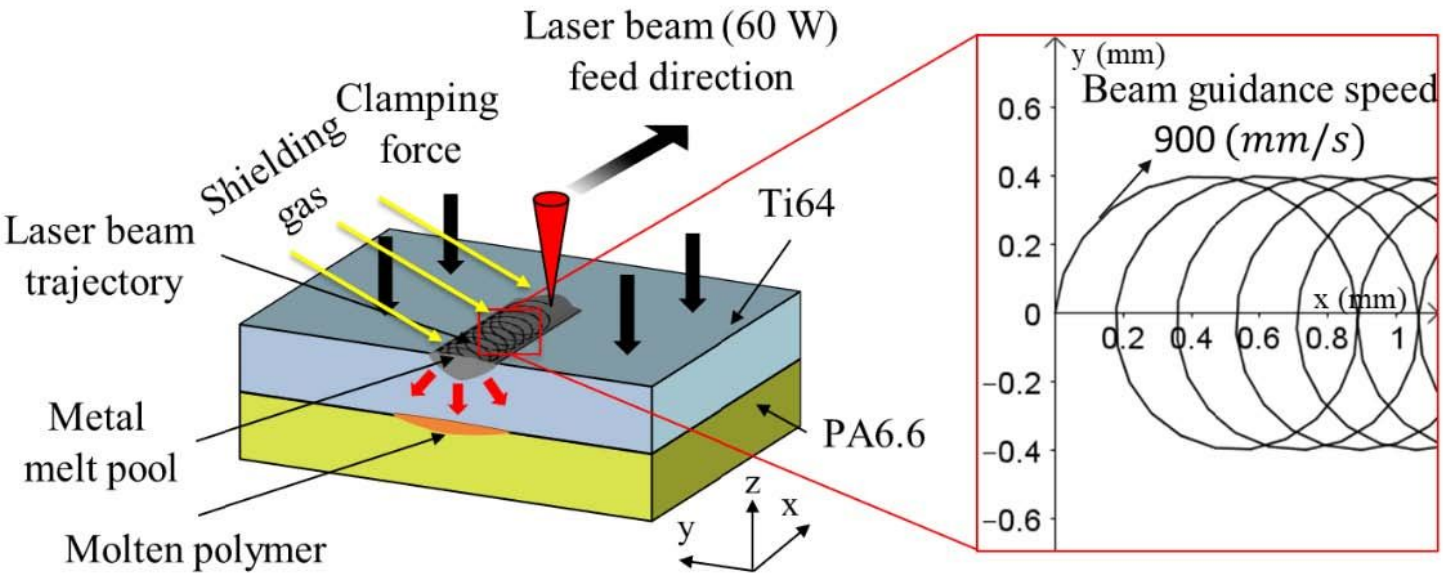

Figure 1

Laser welding setup

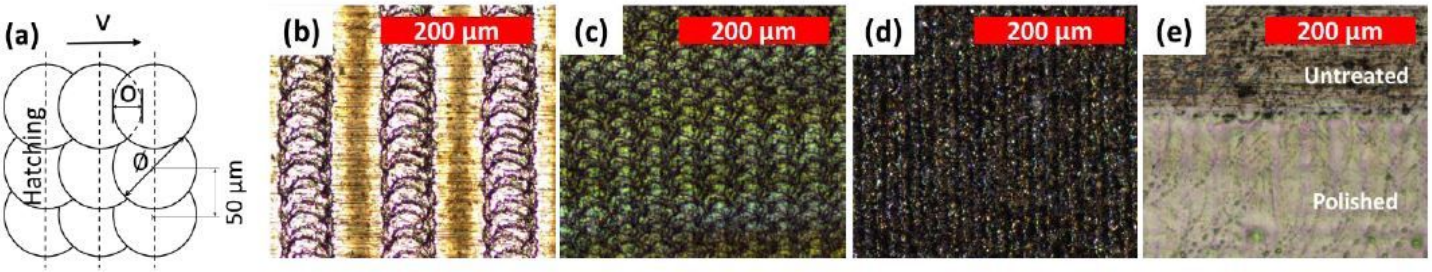

Figure 2

(a) schematic showing ablation parameters on Ti64 surface; (b) patterned ablation; (c) semi-patterned ablation; (d) stochastic ablation; (d) polished ablation.

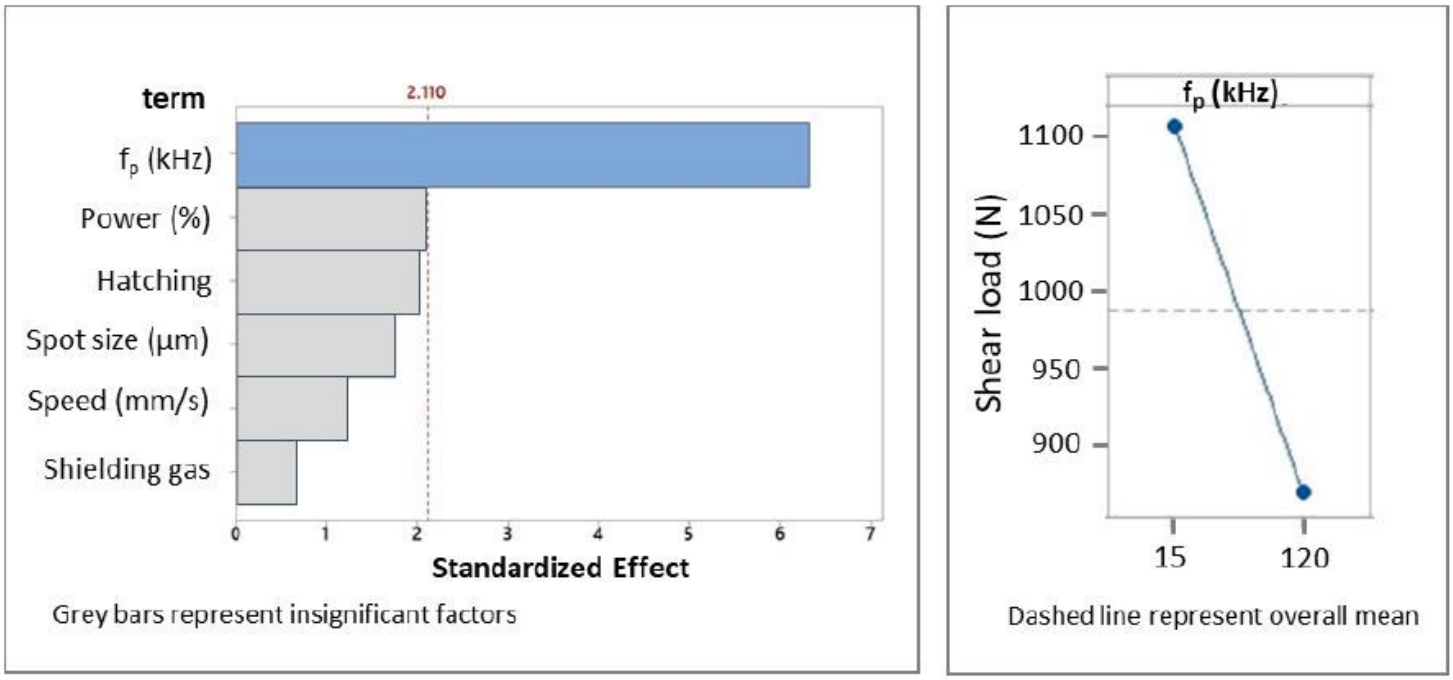

Figure 3

(left) Pareto chart; (right) main effect plot

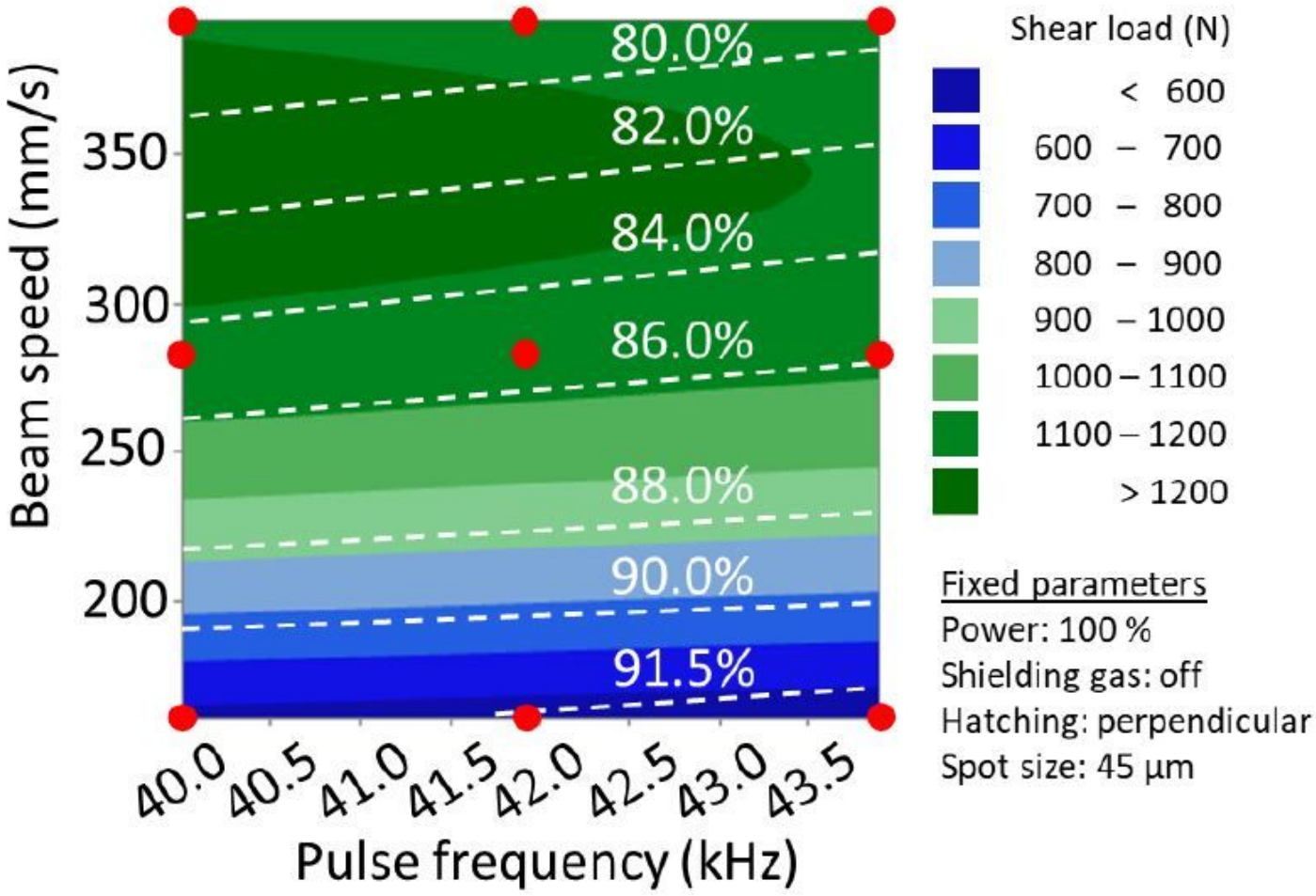

Figure 4

Contour plot of shear load as a function of beam speed and pulse frequency.

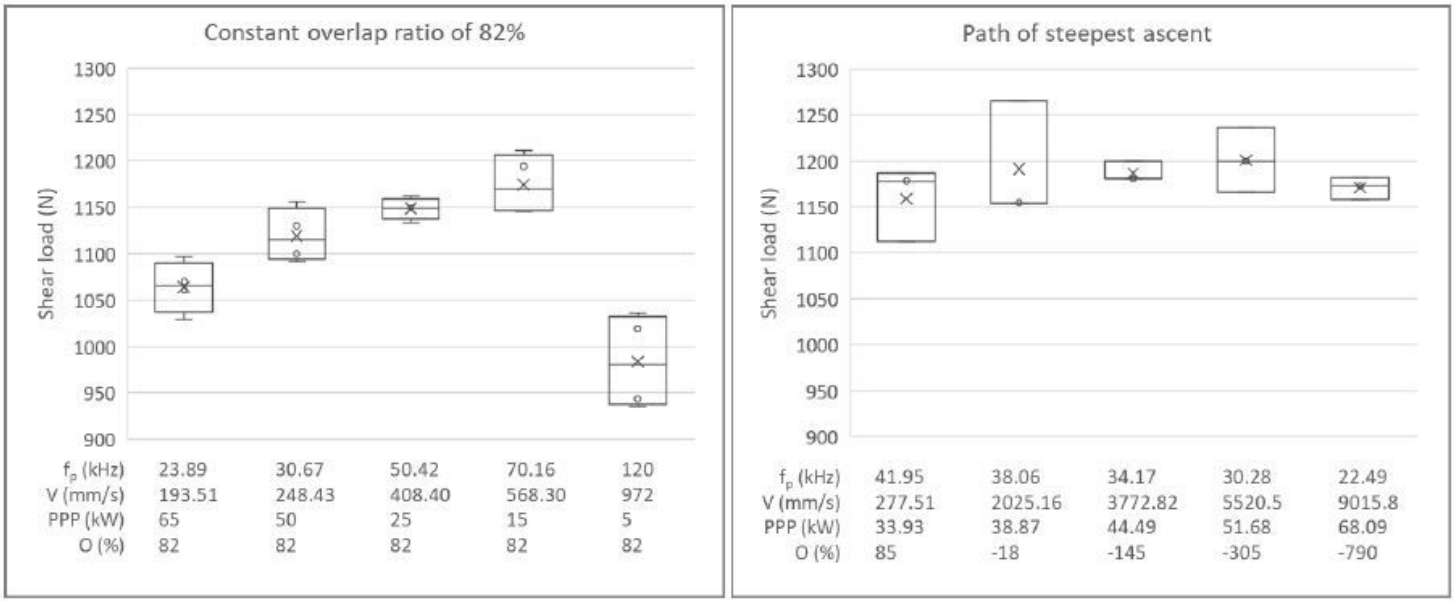

Figure 5

Expanding process window along: (left) 82% overlap ratio; (right) path of steepest ascent

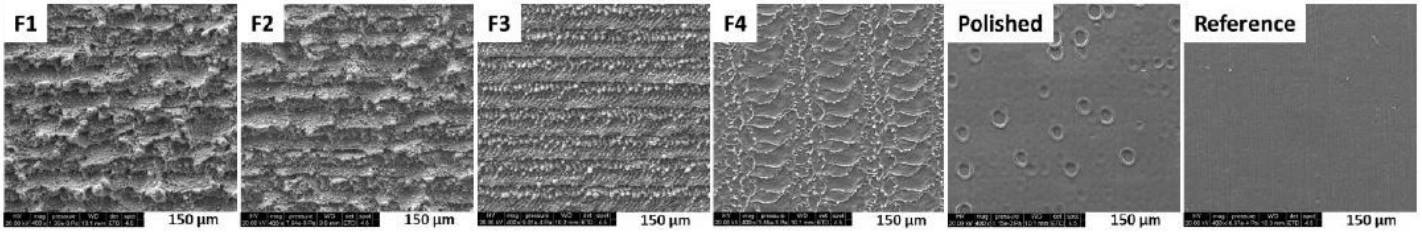

Shear load (N)	387 ± 117	690 ± 57	1064 ± 28	1186 ± 11	764 ± 5	772 ± 70
Fp (kHz)	43.89	40.00	23.89	34.17	120.00	-
V (mm/s)	160.00	160.00	193.50	3772.82	2500.00	-
PPP (kW)	32.00	37.37	65.00	41.70	5.00	-
O (%)	91.89	91.11	82.00	-145.00	53.01	-

Figure 6

effects of ablation parameters on morphology of Ti64 surface